

## Aircraft Performance for Open Air Traffic Simulations

Metz, Isabel; Hoekstra, Jacco; Ellerbroek, Joost; Kugler, D.

**DOI**

[10.2514/6.2016-3522](https://doi.org/10.2514/6.2016-3522)

**Publication date**

2016

**Document Version**

Accepted author manuscript

**Published in**

AIAA Modeling and Simulation Technologies Conference

**Citation (APA)**

Metz, I., Hoekstra, J., Ellerbroek, J., & Kugler, D. (2016). Aircraft Performance for Open Air Traffic Simulations. In *AIAA Modeling and Simulation Technologies Conference: San Diego, USA* [AIAA 2016-3522] American Institute of Aeronautics and Astronautics Inc. (AIAA). <https://doi.org/10.2514/6.2016-3522>

**Important note**

To cite this publication, please use the final published version (if applicable).  
Please check the document version above.

**Copyright**

Other than for strictly personal use, it is not permitted to download, forward or distribute the text or part of it, without the consent of the author(s) and/or copyright holder(s), unless the work is under an open content license such as Creative Commons.

**Takedown policy**

Please contact us and provide details if you believe this document breaches copyrights.  
We will remove access to the work immediately and investigate your claim.

# Aircraft Performance for Open Air Traffic Simulations

Isabel Metz\*, Jacco M. Hoekstra†, Joost Ellerbroek‡, Dirk Kügler§

*Delft University of Technology, 2629 HS Delft, The Netherlands and  
German Aerospace Center DLR, 38108 Braunschweig, Germany*

The BlueSky Open Air Traffic Simulator developed by the Control & Simulation section of TU Delft aims at supporting research for analysing Air Traffic Management concepts by providing an open source simulation platform. The goal of this study was to complement BlueSky with aircraft performance models in order to enable performance-related Air Traffic Management studies. The aircraft performance model developed within this work consists of a kinetic Flight Dynamics Model, which stores the required performance characteristics in a database with type-specific aircraft and engine coefficients. Currently, sixteen commercial turbofan and turboprop aircraft from different range and weight categories are represented. To evaluate the quality of the aircraft performance model, its outputs were compared to results from literature as well as from real flights. It was found that the applied methodologies for the determination of aircraft performance accurately model high-speed drag polars as well as fuel consumption for cruising and taxiing aircraft. The fuel consumption model of climbing and descending aircraft, however, leaves room for improvement. Possible strategies for obtaining a more precise estimation of fuel burn over the entire flight are recommended based on the results of this study. With this work, the BlueSky Open Air Traffic Simulator considers individual aircraft performance. This is an important step in the creation of an open simulation platform for Air Traffic Management research.

## Nomenclature

$AR$	Wing aspect ratio	$S_{ref}$	Wing reference surface area, m <sup>2</sup>
$C$	Thrust-specific fuel consumption, mg/Ns	$T$	Thrust, N
$C_D$	Drag coefficient	$t$	time, s
$C_{D_0}$	Parasite drag	$V_{TAS}$	True airspeed, m/s
$C_f$	Equivalent skin friction coefficient	$\eta_p$	Propeller efficiency
$C_L$	Lift coefficient		
$C_P$	Power-specific fuel consumption, mg/J		
$D$	Drag, N		
$e$	Oswald factor		
$g_0$	Gravitational acceleration, 9.80665 m/s <sup>2</sup>		
$h$	height, m		
$k$	Drag due to lift coefficient		
$M$	Mach number		
$m$	Mass, kg		
$\dot{m}$	Fuel consumption, kg/s		
$P$	Inviscid drag component		
$Q$	Viscous drag component		
$S_{wet}$	Wetted area, m <sup>2</sup>		

---

\*PhD candidate, Institute of Flight Guidance, German Aerospace Center DLR, Lilienthalplatz 7, 38108 Braunschweig, Germany & Control and Simulation Division, Faculty of Aerospace Engineering, Delft University of Technology, 2629 HS Delft, The Netherlands; isabel.metz@dlr.de. AIAA Student Member.

†Professor, Control and Simulation Division, Faculty of Aerospace Engineering, Delft University of Technology, 2629 HS Delft, The Netherlands; j.m.hoekstra@tudelft.nl.

‡Assistant Professor, Control and Simulation Division, Faculty of Aerospace Engineering, Delft University of Technology, 2629 HS Delft, The Netherlands; j.ellerbroek@tudelft.nl.

§Director, Institute of Flight Guidance, German Aerospace Center DLR, Lilienthalplatz 7, 38108 Braunschweig, Germany; dirk.kuegler@dlr.de.

## I. Introduction

To be able to contribute to a modernized Air Traffic Management (ATM) system, research institutes require real- and fast-time simulation environments for evaluating their developed concepts and procedures. To support independent as well as joint research in the area of ATM, the Control & Simulation section of Delft University of Technology (TU Delft) is developing the BlueSky Open Air Traffic Simulator.<sup>1</sup> This simulator enables the visualisation and analysis of air traffic flows as well as ATM concepts. BlueSky is programmed in the open-source language Python and its content is based on open data exclusively. Hence, it can be used and modified without any restrictions or the need for licenses. A detailed description of BlueSky can be found in Ref. 1. The simulator can be downloaded from Ref. 2.

A vital part of an air traffic simulation platform is an aircraft performance model for gaining information about the efficiency and environmental impact of different aircraft procedures. This work complements the BlueSky simulator with an aircraft performance model, which is based on open sources exclusively.

Aircraft manufacturers consider individual aircraft performance characteristics as strictly confidential.<sup>3</sup> As such, existing aircraft performance models usually are available under license agreements only. In order to keep BlueSky an open source simulator, an approach for modelling aircraft characteristics parameters was developed.

One of the best known and widely utilized aircraft performance models for Air Traffic Simulators is the Base of Aircraft Data (BADA), which is provided by the European Organization for the Safety of Air Navigation (EUROCONTROL)<sup>4,5</sup> BADA comes in two levels of accuracy: The BADA family 3 represents aircraft's behaviour within the flight envelope's normal operation part. BADA 4 extends the model to the entire flight envelope and hence needs much more detailed and thus sensible information about aircraft characteristics.<sup>6</sup> This leads to stringent license terms for BADA 4. The accessibility of BADA 3 is divided into two parts: The Flight Dynamics Model (FDM), which relies on basic aeronautics, is described in a freely accessible user manual.<sup>7</sup> The individual aircraft characteristics on the other hand are subject to licenses. The structure of the FDM implemented into BlueSky is compatible with the one of BADA 3. As a result, holders of a BADA 3 license gain the opportunity to operate BlueSky with the BADA 3 aircraft performance models.

As BlueSky is meant to simulate multiple aircraft simultaneously, the developed methods need to be runtime and memory efficient. This ensures a high update frequency of simulations, when handling traffic scenarios with large numbers of aircraft. On the other hand, aircraft performance should be modelled as accurately as possible in order to gain representative results. The challenge of this project was thus to find methods as simple as possible, which lead to adequately precise results.

This paper is organized as follows: In the next paragraph, the structure of the developed performance model is explained. This is followed by a description of the method applied to verify and validate the model's outcome. Finally, the results are presented and the conclusions drawn.

## II. Performance Model Setup

The aircraft performance model described in this paper is based on empirical methods. This takes into account the requirements considering runtime and memory efficiency. Another advantage of empirical methods is, that they can calculate performance parameters with a limited set of input data. This is especially important for BlueSky, as only few aircraft characteristics are publicly available. The calculation process for the relevant performance parameters is visualized in Fig. 1. Its components are described in the following paragraphs.

### II.A. Aircraft and Engine Parameters

The relevant input data for the calculation of the aircraft performance parameters is stored separately for aircraft and engines. This allows to equip a certain aircraft with all engines provided for installation by the manufacturer. As such, the model takes into account variations in performance caused by the different possible airframe-engine combinations, which can be significant.<sup>3</sup> For airframes, the stored data contains information about the applicable engines, weights, geometrical data, the flight envelope and the coefficients for calculating drag. The main source is the Jane's all the World's Aircraft database.<sup>8</sup> The data stored for turbofan engines consists of the rated thrust as well as reference values for fuel

consumption in different stages of flight. This information can all be automatically derived from the regularly updated International Civil Aviation Organization (ICAO) Aircraft Emission Databank.<sup>9</sup> For turboprop aircraft, the engine's power as well as the Power-Specific Fuel Consumption (PSFC), both derived from Jane's Aero Engines<sup>10</sup> are stored.

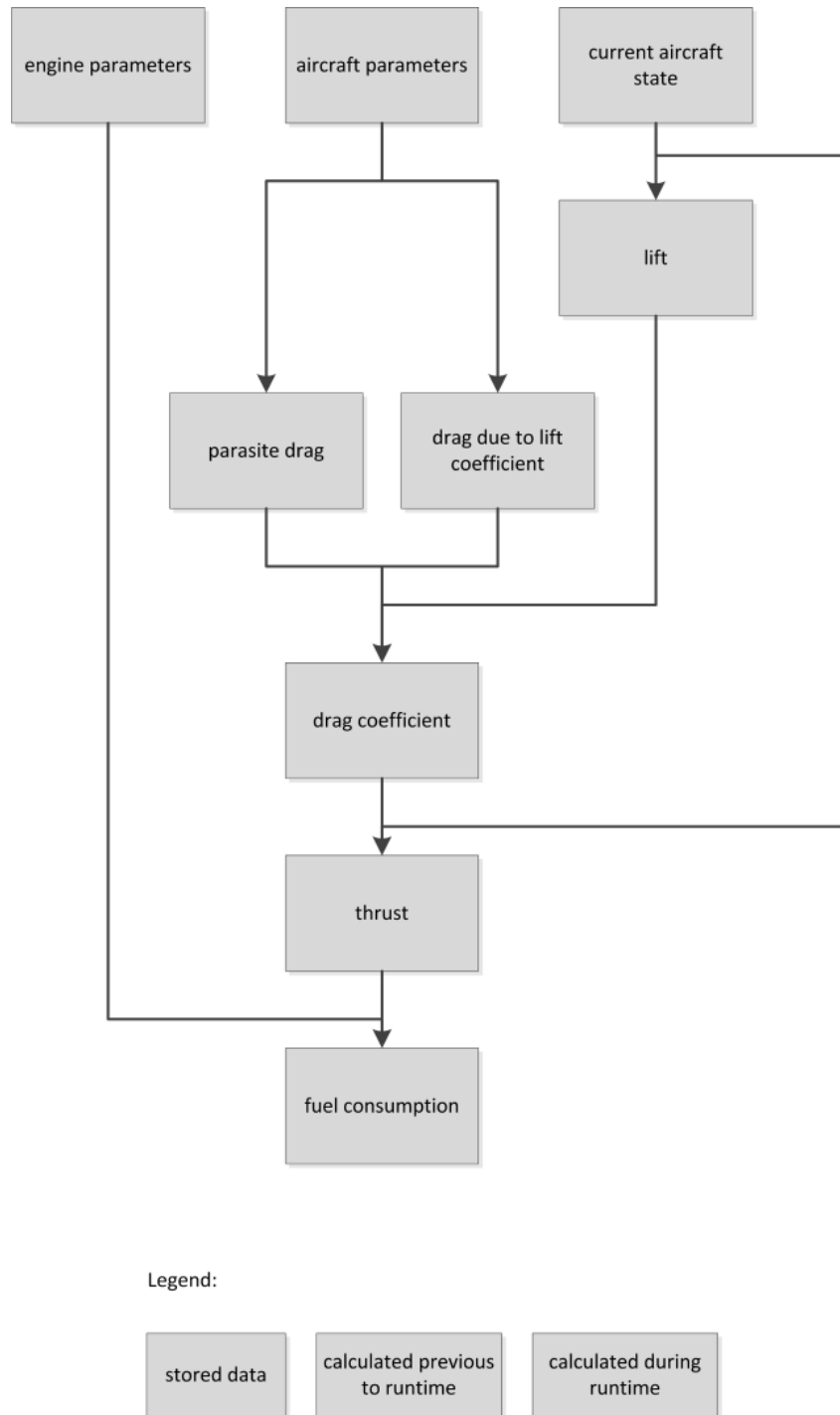


Figure 1: Performance parameter calculation within BlueSky

## II.B. Drag Coefficient

As shown in Eq. (4), the drag coefficient consists of two components: parasite drag and drag due to lift.

$$C_D = \underbrace{C_{D_0}}_{\text{parasite drag}} + \underbrace{k \cdot C_L^2}_{\text{drag due to lift}} \quad (1)$$

where  $C_D$  is the drag coefficient,  $C_{D_0}$  is the parasite drag,  $k$  is the drag due to lift coefficient and  $C_L$  is the lift coefficient.

For the calculation of parasite drag, Eq. (2), introduced by Raymer<sup>11</sup> is applied.

$$C_{D_0} = C_f \cdot \frac{S_{wet}}{S_{ref}} \quad (2)$$

where  $C_f$  is the equivalent skin friction coefficient,  $S_{wet}$  is the wetted area and  $S_{ref}$  is the wing reference surface area.

The values for the equivalent skin friction coefficient as well as the wetted area are approximated from Fig. 2. For aircraft not listed, interpolations between listed aircraft with similar characteristics were performed. Raymer explicitly states that Eq. (2) represents a theoretical approach, which does not take into account increased skin friction due to debris on aircraft's surfaces. Hence, parasite drag is probably slightly underestimated here.

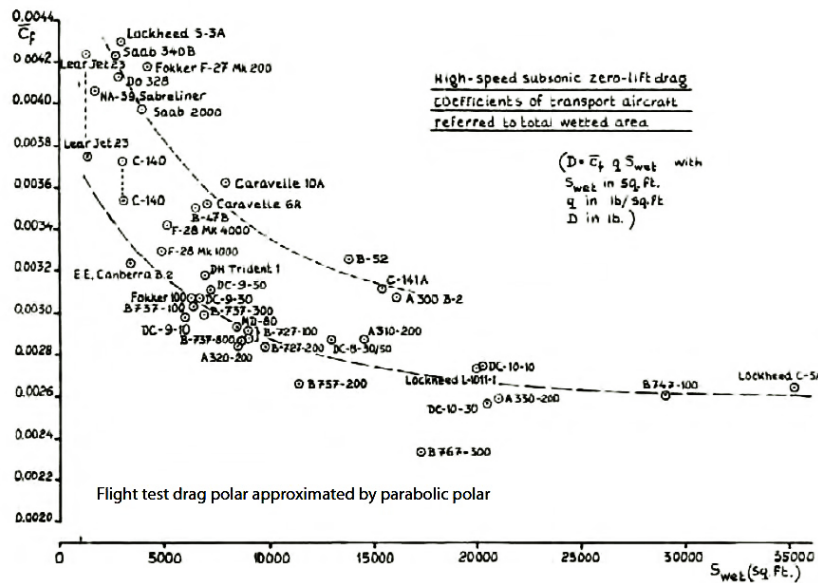


Figure 2: Reference for the estimation of wetted area and equivalent skin friction coefficient (source: Ref. 12)

The second component of the drag coefficient is drag due to lift, which is the product of the drag due to lift coefficient and the square of the lift coefficient. The drag due to lift coefficient  $k$  can be written as

$$k = \frac{Q}{\pi \cdot AR} + P \quad (3)$$

where  $Q$  is the viscous drag component of drag due to lift,  $P$  is the inviscid drag component of drag due to lift and  $AR$  is the aspect ratio. The Oswald factor  $e$  then becomes

$$e = \frac{1}{Q + \pi \cdot AR \cdot P} \quad (4)$$

Based on real flight analysis, Obert<sup>12</sup> provides three numerical solutions for  $P$  and  $Q$ . A statistical evaluation performed for this paper revealed that the values 0.009 for  $P$  and 1.02 for  $Q$  deliver the most accurate results and were thus implemented for the calculation of the drag due to lift coefficient. The applied method can be found in Appendix A.

Using the parasite drag and drag due to lift coefficient calculated previously to runtime, an aircraft's drag coefficient is constantly updated with the current lift during simulation by applying Eq. (4).

The equations above are valid for aircraft in clean configuration. To consider the effect of extracted flaps and landing gear during take-off, initial climb, approach and landing, drag increasing factors are included during those flight phases. Their derivation and integration is explained in Appendix B.

## II.C. Thrust

To calculate an aircraft's current thrust, the previously described components as well as the aircraft's current vertical speed, weight and velocity are fed into the Total Energy Model (TEM). The TEM is a kinetic FDM, which models individual aircraft as point masses, assuming that an aircraft's available energy is exclusively used for change in altitude or velocity.<sup>7</sup> The TEM is given in Eq. (5).

$$(T - D) \cdot V_{TAS} = m \cdot g_0 \cdot \frac{dh}{dt} + m \cdot V_{TAS} \cdot \frac{dV_{TAS}}{dt} \quad (5)$$

where  $T$  is thrust,  $D$  is drag,  $V_{TAS}$  is the true airspeed,  $m$  the aircraft mass,  $g_0$  the gravitational acceleration,  $\frac{dh}{dt}$  corresponds to vertical speed and  $\frac{dV_{TAS}}{dt}$  to longitudinal acceleration.

## II.D. Fuel Consumption

An aircraft's fuel consumption is calculated during runtime via the current thrust and the Thrust-Specific Fuel Consumption (TSFC), as visualized in Eq. (6), obtained from Ref. 11.

$$\dot{m} = T \cdot C \quad (6)$$

where  $\dot{m}$  is the fuel consumption and  $C$  the TSFC

For turbofan aircraft, the TSFC, takes into account Mach and altitude effects as proposed by Raymer<sup>11</sup> and firstly introduced by Mattingly et al.<sup>13</sup> Therefore, Eq. (7) is applied during runtime to update the TSFC based on the current aircraft state.

$$\frac{C}{C_{max}} = \frac{0.1}{\left(\frac{T}{T_{max}}\right)} + \frac{0.24}{\left(\frac{T}{T_{max}}\right)^{0.8}} + 0.66 \cdot \left(\frac{T}{T_{max}}\right)^{0.8} + 0.1 \cdot M \cdot \left[\frac{1}{\left(\frac{T}{T_{max}}\right)} - \left(\frac{T}{T_{max}}\right)\right] \quad (7)$$

where  $C_{max}$  is the TSFC at maximum thrust,  $T_{max}$  is the maximum thrust at the current altitude and  $M$  the Mach number.

Equation (7) is applied for climbing and descending turbofan aircraft. During the taxi and cruise phase, they consume fuel corresponding to values provided by the Aircraft Engine Emission Databank by ICAO.<sup>9</sup> In preliminary studies, this very pragmatic approach for calculating the fuel consumption of taxiing and cruising aircraft has proved to deliver the most accurate results for those flight phases.

Public information about turboprop engine characteristics are strongly limited. Hence, this study employs a very simple approach for calculating fuel consumption of turboprops: It depends on TSFC for all stages of flight. To gain information about a turboprop's TSFC, its PSFC, which is stored in the engine files, is being converted as demonstrated in Eq. (8).

$$C = C_P \cdot \frac{V_{TAS}}{\eta_p} \quad (8)$$

where  $C_P$  is the PSFC and  $\eta_p$  the propeller efficiency, which is set to 0.8 for the BlueSky performance model. This corresponds to the value suggested by Raymer.<sup>11</sup>

The fuel consumption calculation for all aircraft, turbofans and turboprops, is based on uninstalled thrust. Hence, an underestimation of fuel burn has to be expected.<sup>13</sup>

## II.E. Flight Envelope

To ensure that simulated aircraft never operate outside their nominal flight envelope, a flight envelope protection system was implemented into BlueSky. Based on the aircraft characteristics and stage of flight, the flight envelope protection system calculates minimum and maximum velocities, maximum thrust and maximum altitude for each aircraft. Those are then compared to the current target values from the autopilot and, if necessary, the latter are changed to values within the limits for safe flight operations.

### III. Method

The base for evaluating an aircraft's performance is its drag polar. Hence, its precise estimation is vital for further studies. To analyse the method developed for calculating the drag polar within BlueSky, its outcomes were compared to five high-speed drag polars from literature. Interpreting the mean differences between the compared drag polars as measure for the quality of the modelled parasitic drag (linear term of Eq. (4)) and the Pearson coefficient<sup>14</sup> as measure for the quality of the modelled drag due to lift (quadratic term of Eq. (4)), the drag polars were analysed. Fig. 3 exemplary shows the comparison between a Fokker 100 within BlueSky and respective literature data.

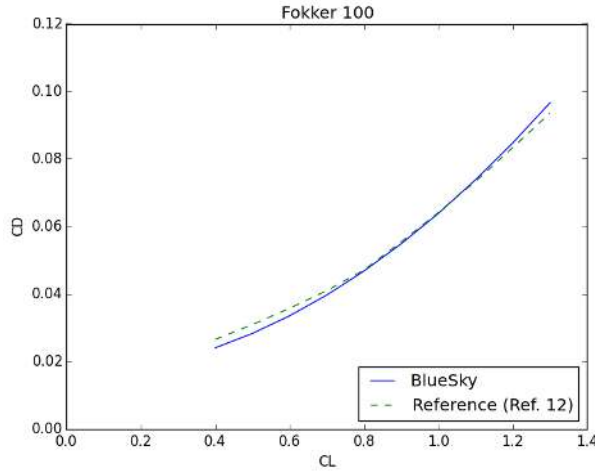


Figure 3: Drag polar comparison for a Fokker 100 aircraft

Based on the initial studies of drag polars, the implemented BlueSky method for fuel consumption was analysed. For this purpose, the flight profile of two real flights performed by an Airbus A320-232 (A320) and a Cessna 550 Citation II (C550) were rebuilt in the simulator and the fuel consumption during the real and the simulated flight compared.

From the data recorded during the real flights, representative segments for climb, cruise and descent were extracted and their trajectories were rebuilt in the BlueSky simulator. An aircraft's trajectory contains its three-dimensional position as well as its current velocity.<sup>15</sup> To achieve the best fits for all the corresponding parameters, some of the default input coefficients for the BlueSky performance model such as bank angle and longitudinal acceleration were adjusted. With this measure, the trajectories and thus the aircraft's performance of the real and simulated flight had the best fit.

The trajectories of the original flights were rebuilt based on the pressure altitude. Wind information provided in the data sets is strongly limited. Hence, it was not considered for the validation. This choice causes no effect on the validation result, because the validation took into account performance over time, which depends on the wind-independent True Airspeed (TAS). Heading changes in the simulations were performed at the same time step as during the real flight to obtain a comparable performance of both aircraft. Due to neglecting the wind influence, this resulted in lateral differences between the flight paths of the real and the simulated aircraft.

To evaluate the fuel consumption during flight, the fuel used for taxi, climb, cruise and descent phase were compared between the real and the simulated aircraft. Thereby, the absolute values for fuel used as well as the relative differences in fuel consumption were considered. The BlueSky model provides a constant fuel flow during ground operations. Hence, it was not necessary to rebuild the ground trajectories for the validation. To obtain the corresponding information for the BlueSky aircraft, the fuel flow during the time the real aircraft spent taxiing was cumulated. As the datasets of both flights end before the taxi phase after landing, only the fuel consumption prior to take-off could be taken into account for the analysis.

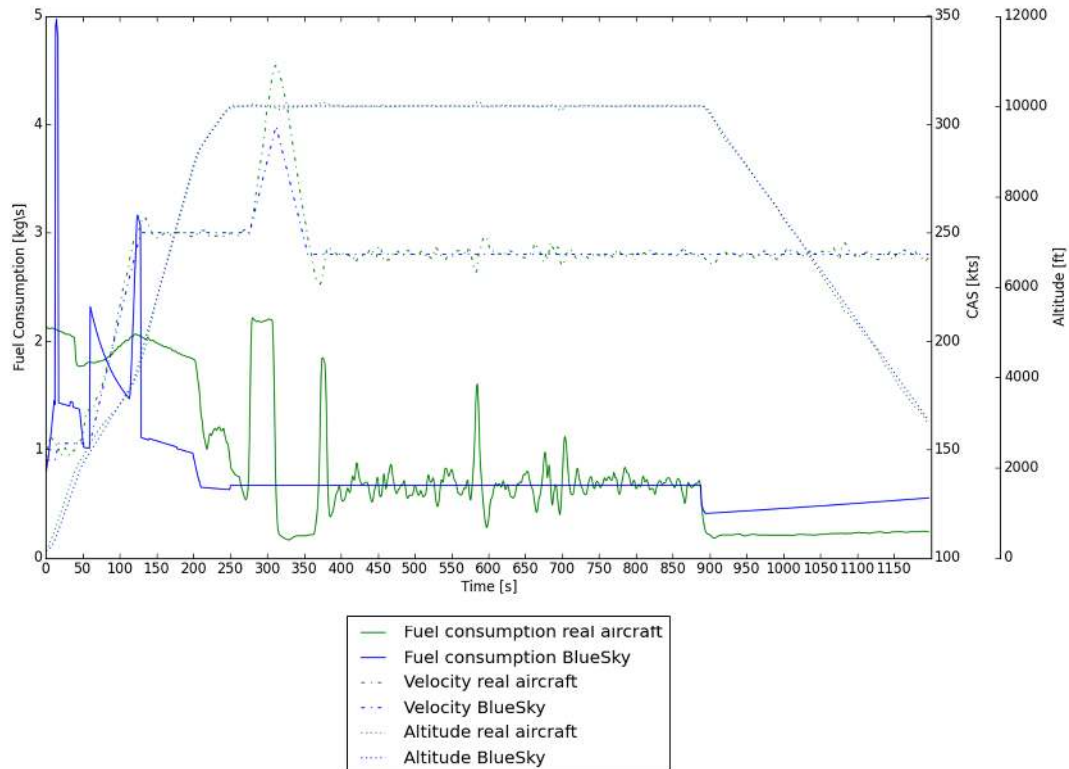


Figure 4: Comparison of the A320 performance in real flight and during simulation

#### IV. Results

The outcome of the drag-polar comparisons contained different results for the aircraft considered. For three of the five compared drag polars, the data used for the implementation into BlueSky and the reference data from literature derive from the same aircraft type generation. The reference data for the other two drag polars originates from older generations than the BlueSky implementation. For the three aircraft, where the compared aircraft type generation is identical, the drag polars strongly correspond: The maximum mean deviation amounts to 7.6 % (standard deviation 2.96 %) and the minimum Pearson coefficient to 0.999995. The correspondence of the drag polars for the remaining two aircraft on the other hand were much lower: The mean deviations are 26.82 % (standard deviation 39.71 %) respectively 23.76 % (standard deviation 2.93 %). For both aircraft, the BlueSky implementation has higher aerodynamic qualities. However, it should be kept in mind, that the aerodynamic qualities of aircraft significantly improved over the last 20 years.<sup>16</sup> Hence, newer generations of aircraft are supposed to produce less drag than their predecessors. Furthermore, the data for both reference aircraft derived from models instead of real flight data, of which one is known to underestimate lift at a certain drag. Hence, the higher aerodynamic qualities of the BlueSky aircraft are in line with the expectations.

The results of the comparison to a further reference - the BADA revision 3.12<sup>7</sup> - support the assumption of an appropriate model for the drag polar within BlueSky. In this analysis, high-speed drag polars for five turbofan and five turboprop aircraft were analysed. The mean difference of all turbofan drag polars amounted to 12.57 % (standard deviation 14.18 %) and to 9.19 % (standard deviation 4.33 %).

Based on the results from the comparison of drag polars, the developed model for fuel consumption within BlueSky was analysed. Therefore, real flights of an A320 and a C550 were considered. Fig. 4 shows the course of velocity, altitude and fuel consumption for the real and simulated flight of the A320.

As visible from Fig. 4, the peaks in fuel consumption due to acceleration or increased climb during the initial climb phase are much higher for the simulated aircraft. As soon as the aircraft climb with constant speed and velocity (from  $t = 150$ s onwards), the gradients of the two aircraft's fuel consumption



Table 1: Differences in fuel consumption [%]

	A320	C550
Taxi	- 8.13	-1.8
Climb	-26.5	-38.24
Cruise	-8.53	-6.92
Descent	+53.31	+1.26

functions becomes almost parallel, whereas BlueSky underestimates the burnt fuel. During level flight, the BlueSky model assumes constant fuel burn and therefore ignores changes in fuel consumption due to velocity changes. In the descent phase, the two fuel functions are similar, whereas the BlueSky model overestimates the consumption significantly. The comparison of the flight profiles of the C550 demonstrated similar behaviour except for the descent phase: Here, the model underestimates the required fuel during the initial climb phase. Only when reducing the rate of descent and setting the approach configuration, overestimation begins. Table 1 summarizes the differences in fuel consumption for the two flights. It can be seen, that except for the descent phase, the model does underestimate fuel consumption for both flights. While the deviations for climbing and descending aircraft vary significantly, the differences during ground and cruise phase lie well below ten percent. The general underestimation of the fuel consumed seems likely, as the BlueSky model does consider uninstalled thrust only and underestimates parasite drag.

## V. Conclusions

The goal of this work was to develop an aircraft performance model for the BlueSky Open Air Traffic Simulator. The model should be based on open sources exclusively and calculate aircraft performance and fuel consumption for individual aircraft as accurately as possible. The results of the comparison of drag polars performed in this study indicate a valid approach for calculating high-speed drag polars, which are the foundation for evaluating aircraft performance. The comparison of fuel consumption demonstrated, that the results of the fuel model implemented into BlueSky are reasonably accurate for taxiing and cruising aircraft even though a constant fuel consumption is assumed. The maximum offset between real and simulated data for these flight phases lies well below ten percent. For climbing and descending aircraft, the differences are significant, especially during changes in velocity or rate of climb/descent.

As BlueSky is designed to simulate multiple aircraft simultaneously, the impact of the aircraft performance model's execution on the entire simulation's efficiency has to be minimal. Studies considering the runtime efficiency of BlueSky including aircraft performance, demonstrated that this additional component still enables a high performance: For a scenario of 500 aircraft, whose performance characteristics are updated with a frequency of 10 Hz, an average runtime of 24.08 ms per update was achieved on a standard laptop <sup>1</sup>.

The resulting set-up of BlueSky enables the performance calculation for turbofan and turboprop aircraft. Currently, ten turbofan and six turboprop aircraft from all range and weight categories are represented. Each of them can be combined with every engine type designated by the manufacturer for the respective aircraft type. Technical guidelines for extending this database are given within simulator's documentation.<sup>17</sup>

The newly developed aircraft performance model serves as a base for the prediction of aircraft performance within BlueSky. Future work should address an improvement in the fuel consumption model for climbing and descending aircraft and taking into account an adjustment for installed thrust and thus higher fuel consumption during all stages of flight. As only two turbofan aircraft were analysed within this study, more data is needed for representative results. Another step to be performed is the evaluation of turboprop data for obtaining information about the validity of their fuel model. Considering the discussed components, it is possible to gain an accurate open source aircraft performance model. For achieving this purpose, TU Delft is currently working on gaining performance data for multiple aircraft out of Automatic Dependent Surveillance Broadcast (ADS-B).<sup>18</sup> With the combination of the empirical methods presented in this paper and performance data of real flights gathered via ADS-B, we are confident to achieve the original ambition of BlueSky: a reliable open source aircraft performance model.

<sup>1</sup>Intel(R) Pentium(R) processor of 2.13 GHz and an installed memory (RAM) of 8.0 GB

## Appendices

### Appendix A: Coefficients for Calculating the Oswald Factor

The Oswald factor within the internal BlueSky performance model is calculated based on the statistical evaluation of lift-dependent drag coefficients of transport aircraft performed by Obert.<sup>12</sup> The underlying relations are given in Eq. (9).

$$e = \frac{1}{Q + P \cdot \pi \cdot AR} \quad (9)$$

where  $e$  is the Oswald factor,  $P$  the inviscid drag component,  $Q$  the viscous drag component and  $AR$  the wing aspect ratio.

Obert provides three numerical combinations for  $P$  and  $Q$ . Based on the information given in Fig. 5 and theoretical values for the Oswald factor gained from Nita and Scholz,<sup>19</sup> these three combinations were compared for eight available commercial aircraft types. The result of this study can be found in Fig. 6. As the combination of  $Q = 1.02$  and  $0.009$  delivers the most accurate overall results, it was chosen for the calculation of the Oswald factor within BlueSky.

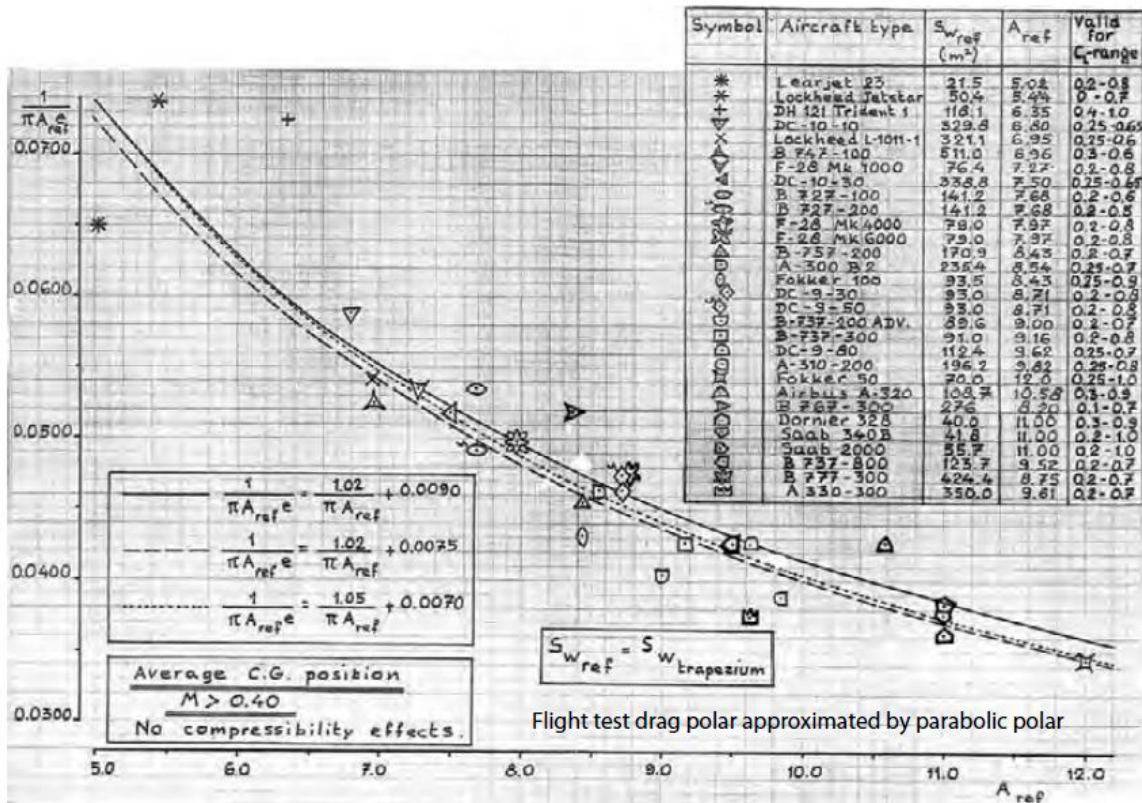


Figure 5: Estimation of the Oswald factor (source: Ref. 12)

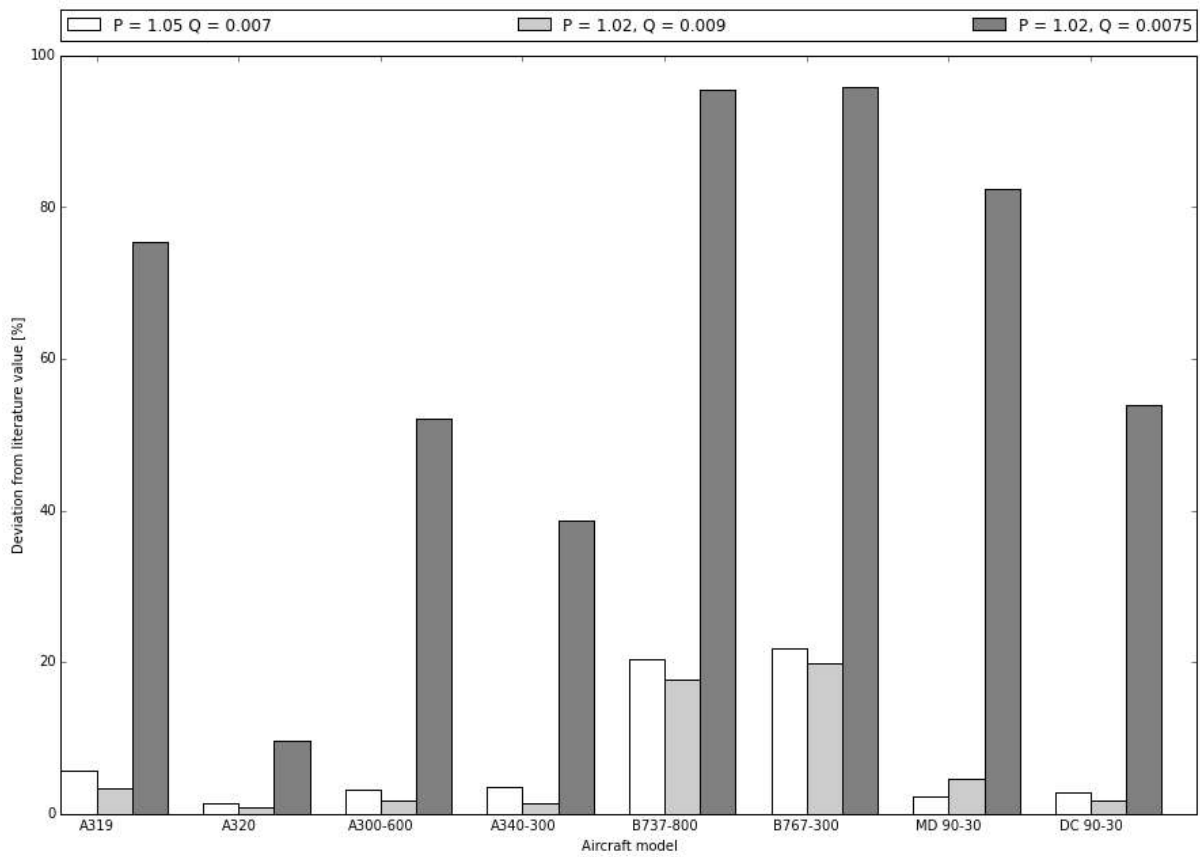


Figure 6: Deviation from the Oswald factor from Ref. 19 for different P-Q-combinations

## Appendix B: Increase in drag for different aircraft configurations

The equations for calculating the drag coefficient's components are valid for clean configuration. For aircraft with extended flaps and landing gear, these parameters have to be increased in order to remain realistic. Roskam<sup>20</sup> provides estimates for the increase in parasite drag and the Oswald Factor, which is an input for drag due to lift. Those increasing factors are visualized in Tables 2 and 3. The numbers provided by Roskam reflect the technological state of the art of the 1980s. To consider the increase in aircraft's aerodynamic qualities since then, the values which lead to the smallest increase in drag are chosen for the implementation in BlueSky. For the increase in parasite drag, this is the minimum value per line, which is added during the flight phases take-off and landing. If both, gear and flaps are extended, their corresponding increases in parasite drag accumulate. For the Oswald factor, the ratio to clean configuration for the largest value per line was calculated. During runtime, the drag due to lift coefficient is multiplied with that value.

For the performance model in BlueSky, it is defined that aircraft taking off retract their gear at 100 ft, the flaps at 400 ft. Landing aircraft extend their flaps at 3000 ft and their gear at 1500 ft. This corresponds with the flight phase definitions in Ref. 7 and Ref. 21.

The chosen approach neglects intermediate flaps settings. Nevertheless, it provides a simple method to extend the drag polar to all flight phases.

Table 2: Increase in zero-lift drag for different aircraft configurations (source: Ref. 20)

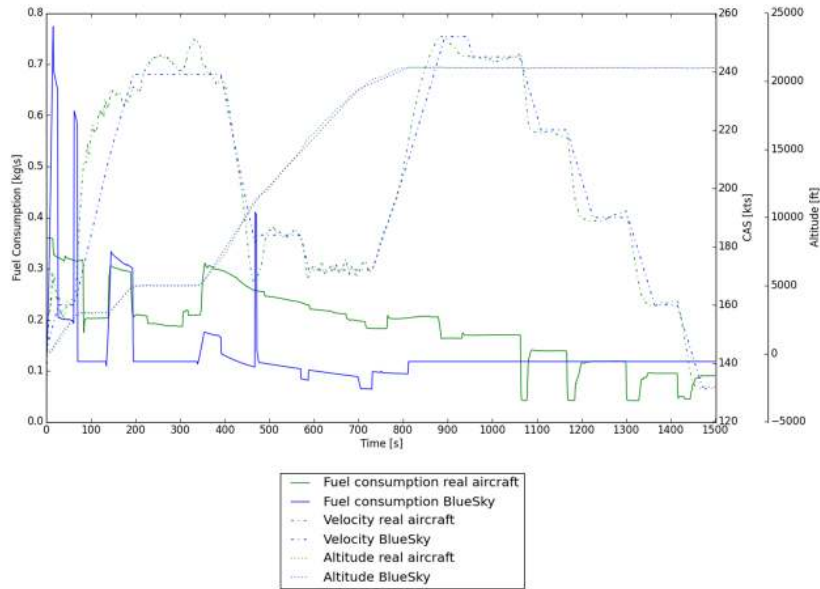
Configuration	Increase in zero-lift drag $\Delta C_{D_0}$ [-]
Clean	0.0
Take-off flaps	0.010 - 0.020
Landing flaps	0.055 - 0.075
Landing gear	0.015 - 0.025

Table 3: Oswald Factor for different aircraft configurations (source: Ref. 20)

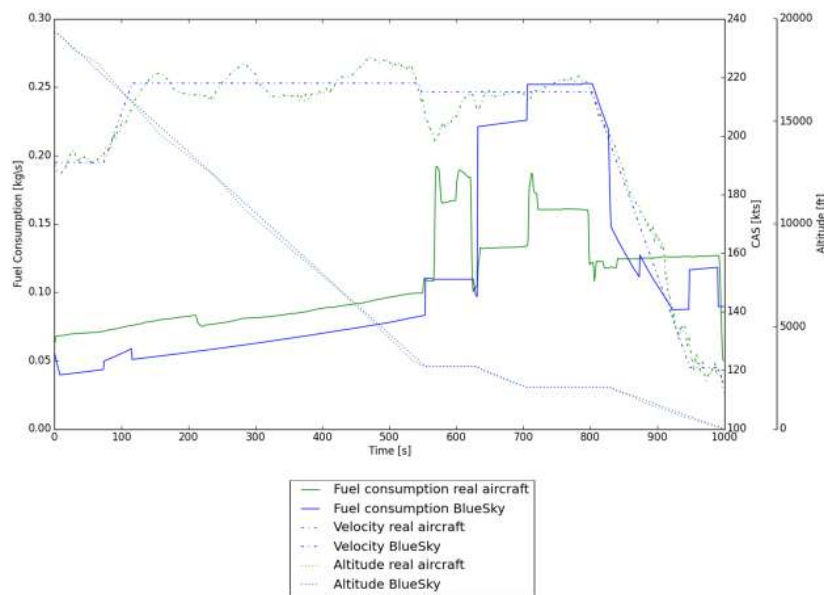
Configuration	Oswald factor $e$ [-]	ratio to clean configuration
Clean	0.8 - 0.85	1.0
Take-off flaps	0.75 - 0.80	0.939
Landing flaps	0.70 - 0.75	0.879
Landing gear	no effect	-

## Appendix C: Validation Results Cessna 550 Citation II

The plots in Fig. 7 visualise the validation results for the flight of the Cessna 550 Citation II. This flight was a test flight including manoeuvres outside the scope of an air traffic simulator. Thus, the part of this flight, where the manoeuvres were performed, was excluded for the validation.



(a) Climb and cruise



(b) Descent

Figure 7: Comparison of the A320 performance in real flight and during simulation

## References

- <sup>1</sup>Hoekstra, J. M. and Ellerbroek, J., “BlueSky ATC simulator project: an open-data and open-source approach,” *Proceedings of the 7th International Conference on Research in Air Transportation*, Philadelphia, PA, USA, June 2016, accepted.
- <sup>2</sup>Hoekstra, J. M., “BlueSky GitHub Repository,” Retrieved 4 November, 2015, from <https://github.com/ProfHoekstra/bluesky>.
- <sup>3</sup>Suchkov, A., Swierstra, S., and Nuic, A., “Aircraft Performance Modelling for Air Traffic Management Applications,” *proceedings of the 5th U.S.A./Europe Seminar on ATM R&D*, Budapest, Hungary, 2003.
- <sup>4</sup>EUROCONTROL, “Base of Aircraft Data (BADA),” 2014, Retrieved 5 November, 2015, from <http://www.eurocontrol.int/services/bada>.
- <sup>5</sup>Holzäpfel, F. et al., “Aircraft wake vortex scenarios simulation package - WakeScene,” *Aerospace Science and Technology*, Vol. 13, 2009, pp. 1–11.
- <sup>6</sup>Poles, D., Nuic, A., and Mouillet, V., “Advanced aircraft performance modeling for ATM: Analysis of BADA model capabilities,” *proceedings of the 29th Digital Avionics Systems Conference (DASC)*, IEEE, Salt Lake City, UT, U.S, October 2010, pp. 1.D.1–1 – 1.D.1–14.
- <sup>7</sup>EUROCONTROL, *User Manual for the Base of Aircraft Data (BADA) Revision 3.12*, EEC Technical/Scientific Report No. 14/04/24-44 ed., 2014.
- <sup>8</sup>IHS, “Jane’s All the World’s Aircraft,” 2015, Retrieved 27 January, 2015, from <https://janes.ihs.com/CustomPages/Janes/ReferenceHome.aspx>.
- <sup>9</sup>ICAO, “Aircraft Emission Databank,” Retrieved 25 February, 2015 from <http://easa.europa.eu/document-library/icao-aircraft-engine-emissions-databank>, February 2014, edition 01/2015.
- <sup>10</sup>IHS, “Jane’s Aero-Engines,” 2015, Retrieved 7 March, 2015, from <https://www.ihs.com/products/janes-aero-engines.html>.
- <sup>11</sup>Raymer, D., *Aircraft Design: A Conceptual Approach*, AIAA Education Series, American Institute of Aeronautics and Astronautics, Inc., Reston, VA, USA, 5th ed., 2012.
- <sup>12</sup>Obert, E., *Aerodynamic Design of Transport Aircraft*, Delft University Press, IOS Press BV, Amsterdam, Netherlands, 2009.
- <sup>13</sup>Mattingly, J., Heiser, W., and Daley, D., *Aircraft Engine Design*, AIAA Education Series, American Institute of Aeronautics and Astronautics, Inc., Washington, D.C., U.S, 4th ed., 1987.
- <sup>14</sup>Dodge, Y., *The Concise Encyclopedia of Statistics*, Springer Science + Business Media, New York, NY, USA.
- <sup>15</sup>EUROCONTROL, “EUROCONTROL ATM Lexicon. One sky - one term,” 2011.
- <sup>16</sup>Flightglobal, “Boeing 747 Aircraft Profile,” Retrieved 5 November, 2015, from <http://www.flightglobal.com/news/articles/boeing-747-aircraft-profile-216270/>, 2015.
- <sup>17</sup>Hoekstra, J. M., “BlueSky Homepage,” Retrieved 4 November, 2015, from <http://homepage.tudelft.nl/7p97s/BlueSky/>.
- <sup>18</sup>Sun, J., Ellerbroek, J., and Hoekstra, J. M., “Large-Scale Flight Phase Identification from ADS-B Data Using Machine Learning Methods,” *Proceedings of the 7th International Conference on Research in Air Transportation*, Philadelphia, PA, USA, June 2016, accepted.
- <sup>19</sup>Nita, M. and Scholz, D., “Estimating the Oswald Factor from Basic Aircraft Geometrical Parameters,” Deutscher Luft- und Raumfahrtkongress, Berlin, Germany, September 2012.
- <sup>20</sup>Roskam, J., *Airplane Desing. Part I: Preliminary Sizing of Airplanes*, Roskam Aviation and Engineering Cooperation, Ottawa, KS, USA, 1989.
- <sup>21</sup>Hünecke, K., *Die Technik des modernen Verkehrsflugzeugs*, Motorbuch Verlag, Stuttgart, Germany, 1st ed., 2008.